Crystals Containing Conformers: A Rare Case in Which a Solid Closely Reflects a Solution Equilibrium Mixture

Enzo Alessio,*,† Ennio Zangrando,† Romeo Roppa,† and Luigi G. Marzilli‡

Dipartimento di Scienze Chimiche, Università di Trieste, 34127 Trieste, Italy, and Department of Chemistry, Emory University, Atlanta, Georgia 30322

Received January 22, 1998

The factors influencing the structural, energetic and dynamic chemistry of complexes with coordinated aromatic N-donor ligands (L) are not well understood. Complexes of the type *cis,cis,cis*-$RuCl_2(Me_2SO)_2$(L1)(L2) with L1 = L2 and L1 ≠ L2 (L1 trans to Cl, L2 trans to Me_2SO) have afforded highly informative results. Here we report studies on two such complexes. One complex provides a rare example of a compound in which the solid state closely reflects the solution state, both in the structure of species involved in a conformational equilibrium and in the position of that equilibrium. In effect, the components of a fluxional equilibrium in solution are trapped, almost unchanged, in the solid state. Specifically, the complex *cis,cis,cis*-$RuCl_2(Me_2SO)_2$(3,5-lut)(1,2-Me_2Im) (**2**) (L1 = 3,5-lut = 3,5-lutidine; L2 = 1,2-Me_2Im = 1,2-dimethylimidazole) exists as two conformers (**R1** and **R2**) in solution and in the solid state (ratio = 0.63(2):0.37(2)); these rotamers differ by a 180° rotation of 1,2-Me_2Im about the Ru−N bond. The orientations of 3,5-lut and 1,2-Me_2Im found in the solid state explain the solution data well, both in terms of ^{1}H NMR chemical shift dispersion and rotation rate of the N-donor ligands. However, there is a displacement of the 1,2-Me_2Im toward the 3,5-lut in the less abundant conformer **R2** in the solid (N(1)−Ru−N(2) angle 78.1(3)° in **R2** vs 93.5(2)° in **R1**); this clear feature in the solid is a type of result that cannot normally be derived from solution investigations or from the study of one conformer in the solid state. Although *cis,cis,cis*-$RuCl_2(Me_2SO)_2$(1,2-Me_2Im)(Me_3Bzm) (**1**) (Me_3Bzm = 1,5,6-trimethylbenzimidazole) exists as a mixture of dynamic rotamers in solution, the crystal structure is typical and reveals the presence of just the rotamer shown to be most abundant by NMR methods. **1** crystallizes in the triclinic space group $P\bar{1}$, Z = 2, with a = 8.863(4) Å, b = 11.907(6) Å, c = 12.406(6) Å, α = 74.32(4)°, β = 83.27(4)°, and γ = 88.89(3)°; **2** in the orthorhombic space group *Pbca*, Z = 8, with a = 12.587(2) Å, b = 12.329(3) Å, and c = 28.382(5) Å. With the added results from this study, it is now clear that the *cis,cis*-$RuCl_2(Me_2SO)_2$ moiety maintains a relatively fixed arrangement that appears also to dominate in solution. The stability of this arrangement is sufficient that the strain evident in the structures appears to be relieved by displacement of the L ligands.

Introduction

The ordered nature of most crystals permits precise determination of structural features in the solid state by diffraction methods. However, almost always, only one of a mixture of conformers present in solution can be accommodated in such ordered arrays. All information on the nature of solution equilibria between distinct, interconverting isomers is lost in the solid state. In particular, the features of the less stable species can rarely be assessed in the solid, and in such cases, information on these less stable species is lost. The position of equilibria and the rates and pathways of dynamic equilibria can be determined in considerable detail by powerful methods such as NMR spectroscopy.[1] However, NMR spectroscopy cannot normally be used to determine precise geometries. We have had to rely on the solid-state structural data of only the stable conformer in a mixture to interpret solution NMR data (NOE cross-peaks, shift dispersion).[2−5]

In complexes of the type *cis,cis,cis*-$RuCl_2(Me_2SO)_2$(L1)(L2) with L1 and L2 = aromatic N-donor ligands (L1 trans to Cl, L2 trans to Me_2SO; Chart 1), rotation of L1 and L2 about the Ru−N bond can be slow at room temperature, thus generating a number of rotamers observable by NMR spectroscopy.[2−4] C_2-symmetric ligands such as pyridine (py) or 3,5-lutidine (3,5-lut), in equilibrium between degenerate orientations, generate topomers, while non-C_2-symmetric (lopsided) ligands such as 1,5,6-trimethylbenzimidazole (Me_3Bzm) and 1,2-dimethylimidazole (1,2-Me_2Im) generate diastereotopomers. Thus when L1 = L2 = a C_2-symmetric ligand, there is only one possible rotamer, but when these are lopsided, there are four possible rotamers (Chart 2). When L1 ≠ L2, there are two geometrical isomers, each with zero, two, and four likely rotamers when, respectively, zero, one, and two of the L's are lopsided.

Hence, the *cis,cis,cis*-$RuCl_2(Me_2SO)_2$(L1)(L2) class of coumpounds has a wealth of informative dynamic, spectral, and

* To whom correspondence should be addressed. Contact address: Dipartimento di Scienze Chimiche, Università di Trieste, Via Giorgieri 1, 34127 Trieste, Italy. Phone: +39 40 6763961. Fax: +39 40 6763903. E-mail: alessi@uts.univ.trieste.it.

† Università di Trieste.

‡ Emory University.

(1) (a) Perrin, C. L.; Dwyer, T. J. *Chem. Rev.* **1990**, *90*, 935. (b) Orrell, K. G.; Sik, V. *Annu. Rep. NMR Spectrosc.* **1987**, *19*, 79. (c) Shokhirev, N. V.; Shokhireva, T. Kh.; Polam, J. R.; Watson, C. T.; Raffii, K.; Simonis, U.; Walker, F. A. *J. Phys. Chem. A* **1997**, *101*, 2778. (d) Momot, K. I.; Walker, F. A. *J. Phys. Chem. A* **1997**, *101*, 2787.

(2) Marzilli, L. G.; Iwamoto, M.; Alessio, E.; Hansen, L.; Calligaris, M. *J. Am. Chem. Soc.* **1994**, *116*, 815.

(3) Iwamoto, M.; Alessio, E.; Marzilli, L. G. *Inorg. Chem.* **1996**, *35*, 2384.

(4) Alessio, E.; Calligaris, M.; Iwamoto, M.; Marzilli, L. G. *Inorg. Chem.* **1996**, *35*, 2538.

(5) Alessio, E.; Hansen, L.; Iwamoto, M.; Marzilli, L. G. *J. Am. Chem. Soc.* **1996**, *118*, 7593.

S0020-1669(98)00066-4 CCC: $15.00
Published on Web 04/30/1998

Chart 1. Labeling for the Octahedral Ru Complexes Ligand Positions

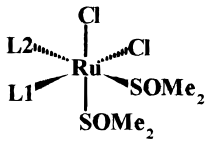

Chart 2. Representations of the Four Possible Diastereotopomers, Two HH and Two HT, That Can Occur in *Cis,Cis,Cis* Octahedral Ru Complexes Bearing Two Lopsided Ligands (Indicated with Arrows)

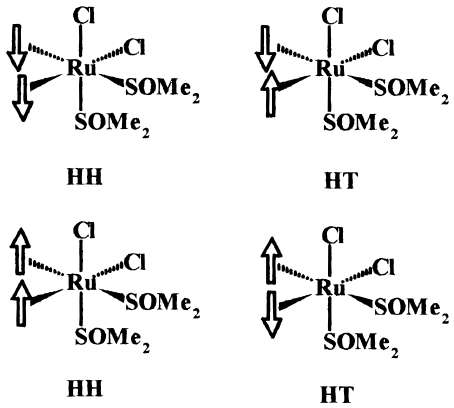

structural features; understanding these closely interwoven features is of general interest in inorganic and bioinorganic chemistry.

We previously described the solution dynamic behavior of *cis,cis,cis*-$RuCl_2(Me_2SO)_2(1,2\text{-}Me_2Im)_2$, which is characterized by the slow, independent rotation of both nitrogen ligands between two orientations at 180° from each other, thus generating all four likely diastereotopomers, two head-to-head (HH) and two head-to-tail (HT).[3] In contrast, *cis,cis,cis*-$RuCl_2(Me_2SO)_2(Me_3Bzm)_2$ exists in solution as only two diastereotopomers; one of these is found in the solid state. In the latter compound and also in *cis,cis,cis*-$RuCl_2(Me_2SO)_2(py)(Me_3Bzm)$, formally obtained upon replacement of Me_3Bzm trans to Cl with a pyridine, NMR data indicated that the Me_3Bzm trans to Me_2SO does not rotate in solution.[4] These data and X-ray crystal data showed that in both complexes such Me_3Bzm had the same orientation, with the mean plane of the ligand almost bisecting the Cl(1)−Ru−Cl(2) angle and H(2), the proton bound to the carbon atom between the two N atoms, nearly equidistant from the two Cl atoms. This fixed position of the Me_3Bzm likely results from the electrostatic interactions between the δ^+ H(2) and the cis halides. These results along with other data[5] have led us to suggest that this electrostatic effect can have wide implications in metallobiochemistry, including effects in adducts of anticancer drugs with DNA where the attack site is the imidazole ring of purine nucleobases.[6]

In this paper we continue to explore the dynamic and structural features of *cis,cis,cis*-$RuCl_2(Me_2SO)_2(L1)(L2)$ compounds; in particular, we report the structural characterization of *cis,cis,cis*-$RuCl_2(Me_2SO)_2(1,2\text{-}Me_2Im)(Me_3Bzm)$ (**1**) and *cis,cis,cis*-$RuCl_2(Me_2SO)_2(3,5\text{-lut})(1,2\text{-}Me_2Im)$ (**2**), together with the dynamic behavior of the latter.

Experimental Section

Reagents. Analytical grade solvents and DMSO were used without further purification. All reagents, including $CDCl_3$, were from Aldrich.

Starting Materials. *cis*-$RuCl_2(Me_2SO)_4$ and *cis,cis,cis*-$RuCl_2(Me_2SO)_2(1,2\text{-}Me_2Im)(Me_3Bzm)$ (**1**) were prepared by known methods.[3] Crystals of **1** suitable for X-ray investigation were obtained by recrystallization of the crude products from chloroform/DMSO mixtures upon addition of diethyl ether (Anal. Calcd for $C_{19}H_{32}Cl_2N_4O_2RuS_2$ (MW 584.60): C, 39.04; H, 5.52; N, 9.58. Found: C, 39.1; H, 5.54; N, 9.59). *cis,fac*-$RuCl_2(Me_2SO)_3(3,5\text{-lut})$ was prepared by a method analogous to that described in ref 4 for *cis,fac*-$RuCl_2(Me_2SO)_3(py)$.

***cis,cis,cis*-$RuCl_2(Me_2SO)_2(3,5\text{-lut})(1,2\text{-}Me_2Im)$ (2).** 1,2-Me_2Im (0.3 mL, 3.4 mmol) was added to a suspension of *cis,fac*-$RuCl_2(Me_2SO)_3(3,5\text{-lut})$ (1.0 g, 2 mmol) in absolute ethanol (30 mL). When heated at reflux for 20 min, the magnetically stirred suspension became a clear, yellow solution. The volume was reduced to ∼2 mL by rotary evaporation. The yellow microcrystalline precipitate which slowly formed after addition of diethyl ether was collected by filtration, rapidly washed with cold ethanol and diethyl ether, and vacuum-dried at 25 °C (yield 0.42 g, 45%). As shown by NMR crude **2** contained *cis,cis,cis*-$RuCl_2(Me_2SO)_2(1,2\text{-}Me_2Im)_2$ and also *cis,cis,cis*- and *trans,cis,cis*-$RuCl_2(Me_2SO)_2(3,5\text{-lut})_2$ impurities. Pure **2** (by NMR) was obtained from the raw product after three recrystallizations from acetone/DMSO mixtures (0.25 g in 5 mL of acetone and 0.1 mL of DMSO) upon careful addition of diethyl ether at room temperature (yield of each recrystallization 75%). Anal. Calcd for $C_{16}H_{29}Cl_2N_3O_2RuS_2$ (MW = 531.51): C, 36.15; H 5.50; N, 7.90. Found: C, 35.9; H, 5.51; N, 7.87.

NMR Spectroscopy. ^1H NMR experiments were performed in $CDCl_3$ at 400 MHz on a JEOL EX400 spectrometer equipped with a variable-temperature unit. Spectra were typically collected with a 6000 Hz spectral window, a 30° pulse, and 32K data points. Sample concentration vaied from 30 to 100 mM. All spectra were referenced to TMS.

For the 2D $^1H-^1H$ EXSY/NOESY experiments a 512 × 1024 data matrix was collected with 32 scans per t_1 increment (16 scans for the low-*T* experiments). Each acquisition was preceded by four dummy scans and a 1 s relaxation delay. The second dimension was zero filled to 1024 data points prior to Fourier transformation. A mixing time of 500 ms was used in all experiments and implemented along with spectral windows in the range 3100−3500 Hz, depending on the complex. The pulse delay was 2.35 s. A square sine bell function with no phase shift was applied in both dimensions.

X-ray Data Collections and Structure Determinations. Single-crystal data collections for **1** and **2** were performed at 293(2) K with an Enraf-Nonius CAD4 single-crystal diffractometer equipped with graphite monochromator and Mo Kα radiation ($\lambda = 0.710\ 69$ Å). Cell parameters were refined by 25 randomly selected reflections in the θ range 12−17° for both compounds. Data were collected by the $\omega/2\theta$ scan mode. Intensities were corrected for Lorentz and polarization effects. Absorption corrections were applied via an empirical ψ scan. The structures were solved by conventional Patterson and Fourier methods. In the crystal of **2**, the ΔF map revealed two coplanar orientations for the 1,2-Me_2Im ligand with the *N*-methyl (C(14)) shared by both rotamers. The occupancy factors ratio for the two conformers were refined to 0.63(2)/0.37(2). Structure **1** was refined against F_o by using the MOLEN package,[7] while structure **2** was refined against F_o^2 with the program SHELXL93.[8] All non-H atoms, except those of the 1,2-Me_2Im at lower occupancy of **2**, were refined with anisotropic thermal parameters. The contribution of the H atoms were included at calculated positions in final cycles of refinements, excluding those of the disordered 1,2-Me_2Im of **2**. Crystal data and details of refinements are summarized in Table 1.

Results

The crystal structure of *cis,cis,cis*-$RuCl_2(Me_2SO)_2(1,2\text{-}Me_2Im)(Me_3Bzm)$ (**1**) reaffirms the ligand disposition previously established by NMR,[3] with 1,2-Me_2Im trans to Cl and Me_3Bzm trans to Me_2SO (Figure 1).

(6) Marzilli, L. G.; Marzilli, P. A.; Alessio, E. *Pure Appl. Chem.*, in press.

(7) *MOLEN, An Interactive Structure Solution Procedure*; Enraf-Nonius: Delft, The Netherlands, 1990.

(8) Sheldrick, G. M. *SHELXL-93, Program for crystal structure refinement*; Universität Göttingen: Göttingen, Germany, 1993.

Table 1. Crystallographic Data for **1** and **2**

	1	**2**
chem formula	$C_{19}H_{32}RuCl_2S_2O_2N_4$	$C_{16}H_{29}RuCl_2S_2O_2N_3$
fw	584.60	531.51
space group	$P\bar{1}$ (No. 2)	*Pbca* (No. 61)
a, Å	8.863(4)	12.587(2)
b, Å	11.907(6)	12.329(3)
c, Å	12.406(6)	28.382(5)
α, deg	74.32(4)	90.00
β, deg	83.27(4)	90.00
γ, deg	88.89(3)	90.00
V, Å^3	1252(1)	4404(2)
Z	2	8
T, °C	20	20
λ, Å	0.710 69	0.710 69
ρ_{calcd}, g cm^{-3}	1.55	1.60
μ(Mo Kα), cm^{-1}	10.1	11.6
$R(F_o)$[a]	0.032	0.043
R_w[a]	0.037	0.108

[a] $R = (\sum||F_o| - |F_c||)/\sum|F_o|$; $R_w = [(\sum w(|F_o| - |F_c|)^2/\sum w(F_o)^2]$ for **1**; $R_w = [(\sum w(F_o^2 - F_c^2)^2/\sum w(F_o^2)^2]^{1/2}$ for **2**.

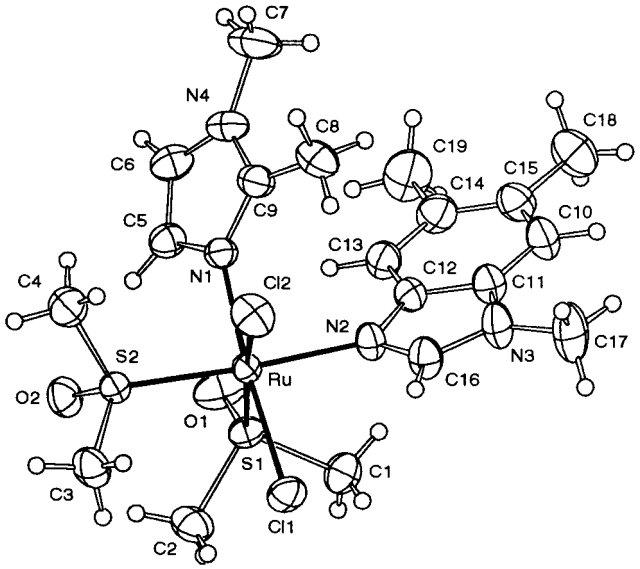

Figure 1. ORTEP drawing and atom-labeling scheme (thermal ellipsoids at 50% probability) of *cis,cis,cis*-$RuCl_2(Me_2SO)_2$(1,2-Me_2Im)-(Me_3Bzm) (**1**).

The ^{1}H NMR spectrum of the complex was in agreement with the presence of only two of the four possible diastereotopomers, one HH and one HT in a ∼1:5 ratio; these interconvert through slow rotation of 1,2-Me_2Im, while Me_3Bzm was unable to rotate.[3] The X-ray structure demonstrates that the orientation of the two lopsided ligand in the solid state is HT and therefore corresponds qualitatively to that of the most abundant rotamer in solution. The plane of Me_3Bzm (coplanar within 0.018 Å) is oriented with the head, represented by H(2) on C(16) (Figure 1), pointing between the Cl atoms, as found in *cis,cis,cis*-$RuCl_2(Me_2SO)_2$(py)(Me_3Bzm) and *cis,cis,cis*-$RuCl_2(Me_2SO)_2(Me_3Bzm)_2$. The 1,2-$Me_2$Im ligand (coplanar within 0.007 Å, excluding the methyl groups) is oriented with the plane between the S atoms and the head, defined as the H(4) end of the ligand on C(5) (Figure 1), toward the S atoms.

The complex shows coordination bond lengths and angles (Table 2) close to those observed in the *cis,cis,cis*-$RuCl_2(Me_2SO)_2$(py)(Me_3Bzm) and *cis,cis,cis*-$RuCl_2(Me_2SO)_2(Me_3Bzm)_2$.[4] Both bases show an unsymmetrical coordination to the metal, with the parameters for the ligating N atoms highly distorted from trigonal geometry. In fact the Ru−N(1)−C(5) and Ru−N(1)−C(9) angles are 122.6(2) and 131.1(2)°, while Ru−N(2)−C(12) and Ru−N(2)−C(16) are 130.5(2) and 123.8(3)°, respectively. The distortion of Me_3Bzm is similar to that found for the corresponding ligand in *cis,cis,cis*-$RuCl_2(Me_2SO)_2$(py)(Me_3Bzm) (Ru−N(2)−C(12) 131.4(1)°) and in *cis,cis,cis*-$RuCl_2(Me_2SO)_2(Me_3Bzm)_2$ (Ru−N(2)−C(12) 128.5(2)°).[4]

Table 2. Selected Bond Distances (Å), Angles (deg), and Torsion Angles (deg) for **1** and **2**

	1	**2**[a]
Ru−N(1)	2.113(3)	2.116(4)
Ru−N(2)	2.122(3)	2.118(7) [2.191(12)]
Ru−S(1)	2.2536(9)	2.251(2)
Ru−S(2)	2.237(1)	2.252(2)
Ru−Cl(1)	2.4111(8)	2.416(2)
Ru−Cl(2)	2.433(1)	2.435(2)
N(1)−Ru−N(2)	88.0(1)	93.5(2) [78.1(3)]
N(1)−Ru−S(1)	96.12(8)	97.27(13)
N(2)−Ru−S(1)	90.41(9)	94.1(2) [83.3(3)]
N(1)−Ru−S(2)	88.58(9)	88.79(12)
N(2)−Ru−S(2)	175.87(8)	171.3(2) [166.1(3)]
S(1)−Ru−S(2)	92.21(3)	93.87(6)
N(1)−Ru−Cl(1)	175.03(8)	176.12(13)
N(2)−Ru−Cl(1)	87.86(7)	84.7(2) [100.8(3)]
S(1)−Ru−Cl(1)	86.59(3)	86.27(6)
S(2)−Ru−Cl(1)	95.49(3)	92.58(6)
N(1)−Ru−Cl(2)	91.16(8)	89.93(13)
N(2)−Ru−Cl(2)	89.14(9)	83.3(2) [96.2(3)]
S(1)−Ru−Cl(2)	172.69(3)	172.51(6)
S(2)−Ru−Cl(2)	88.67(4)	88.32(6)
Cl(1)−Ru−Cl(2)	86.10(3)	86.48(6)
N(2)−Ru−N(1)−C(5)	129.1(3)	129.6(5)
N(2)−Ru−N(1)−C(9)	−41.0(3)	−52.6(5)
N(1)−Ru−N(2)−C(12)	−33.1(3)	−39.6(8) [141(1)]
N(1)−Ru−N(2)−C(16)	136.5(3)	137.6(7) [−40(1)]

[a] Values in square brackets pertain to 1,2-Me_2Im at low occupancy (N(2a)).

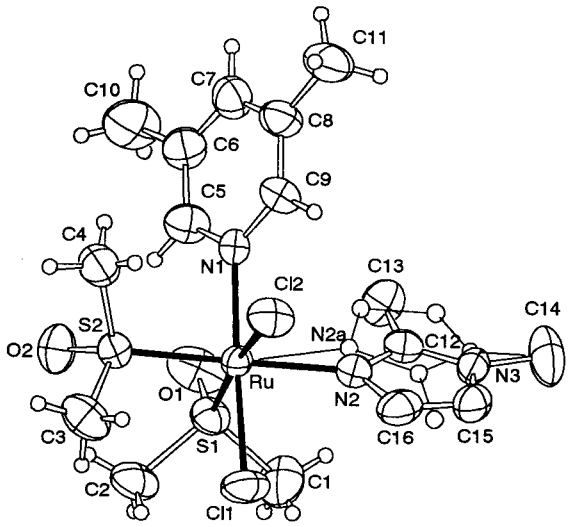

Figure 2. ORTEP drawing and atom-labeling scheme (thermal ellipsoids at 50% probability) of *cis,cis,cis*-$RuCl_2(Me_2SO)_2$(3,5-lut)(1,2-Me_2Im) (**2**). The two orientations assumed by 1,2-Me_2Im are shown, and the less abundant rotamer is represented with small-sized atoms.

The compound *cis,cis,cis*-$RuCl_2(Me_2SO)_2$(3,5-lut)(1,2-Me_2Im) (**2**) was obtained by treatment of *cis,fac*-$RuCl_2(Me_2SO)_3$(3,5-lut) with a slight excess of 1,2-Me_2Im in refluxing ethanol. The crystal structure (Figure 2) showed that the symmetrical, six-membered ring of 3,5-lut is trans to Cl, while the more sterically demanding five-membered ring of 1,2-Me_2Im is trans to Me_2SO, i.e., in the less sterically crowded position. NMR spectra of

Table 3. ^{1}H NMR Chemical Shifts (ppm *vs* TMS) of *cis,cis,cis*-$RuCl_2(Me_2SO)_2$(3,5-lut)(1,2-Me_2Im) (**2**) in $CDCl_3$ at Room Temperature

	R1 ("slow")	**R2** ("fast")
3,5-lut		
Hα	8.95 (s, 1H)	8.85 (s, 1H)
Hα'	8.39 (s, 1H)	8.20 (s, 1H)
$(CH_3)\beta$	2.31 (s, 3H)	2.29 (s, 3H)
$(CH_3)\beta'$	2.12 (s, 3H)	2.08 (s, 3H)
Hγ	7.30 (s, 1H)	7.26 (s, 1H)
1,2-Me_2Im		
H(4)	7.81 (m, 1H)	6.10 (m, 1H)
H(5)	6.92 (m, 1H)	6.69 (m, 1H)
1-Me	3.57 (s, 3H)	3.61 (s, 3H)
2-Me	1.61 (s, 3H)	2.92 (s, 3H)
Me_2SO[a]	3.39 (s, 3H)	3.33 (s, 3H)
	2.74 (s, 3H)	2.77 (s, 3H)
Me_2SO[b]	3.72 (s, 3H)	3.68 (s, 3H)
	2.76 (s, 3H)	2.79 (s, 3H)

[a] Me_2SO *trans* to 1,2-Me_2Im. [b] Me_2SO *trans* to Cl.

Table 4. Comparison between the ^{1}H NMR Chemical Shifts (ppm *vs* TMS) of 1,2-Me_2Im *Trans* to Me_2SO in *cis,cis,cis*-$RuCl_2(Me_2SO)_2$(3,5-lut)(1,2-Me_2Im) (**2**) and in *cis,cis,cis*-$RuCl_2(Me_2SO)_2$(1,2-Me_2Im)$_2$ (**3**)[a] in $CDCl_3$

	R1 of **2**	**R1** (HT) of **3**	**R4** (HH) of **3**	**R2** of **2**	**R2** (HH) of **3**	**R3** (HT) of **3**
H(4)	7.81	7.94	7.95	6.10	6.64	6.43
H(5)	6.92	6.94	6.89	6.69	6.81	6.69
1-Me	3.57	3.65	3.59	3.61	3.68	3.64
2-Me	1.61	1.95	1.81	2.92	3.01	3.01

[a] From ref 3.

the crude product contained no evidence of the geometrical isomer of **2** with the two N-donor ligands interchanged; this result is similar to our studies with **1** and with *cis,cis,cis*-$RuCl_2(Me_2SO)_2(py)(Me_3Bzm)$.[4]

In the solid state there are two conformers of **2** (Table 2) that differ by a 180° rotation of the 1,2-Me_2Im about the Ru−N bond. Occupancies of these conformers were refined to 0.63(2) and 0.37(2); in the most abundant one, the 2-Me of 1,2-Me_2Im is oriented toward the 3,5-lut. The crystal packing does not appear to be able to affect the relative abundance of the rotamers. Rotation of 1,2-Me_2Im also induces a slight distortion in the coordination sphere near the lopsided ligand, with a N(2)−Ru−N(2a) angle of 20.1(3)° between the two rotamers, due to the unsymmetrical coordination of imidazole. The Ru−N(2)−C(12) and Ru−N(2)−C(16) angles are 133.1(6) and 120.4(7)°, respectively, in the major rotamer, while they are 132.0(9) and 122.1(10)°, respectively, in the minor one. Most of the coordination bond lengths and angles of **2** (Table 2) are in the range usually found for such complexes.[4]

In both **1** and **2** the mutual orientation of the two N-ligands is represented by the dihedral angle between the mean planes of the ligands (43.8(3)° in **1** and ∼66° in **2**, both orientations) and by the torsion angles reported in Table 4.

The ^{1}H NMR spectrum of **2** in several solvents at 20 °C has twice the number of signals expected for one conformer. The signals can be grouped rather easily into two sets (arbitrarily labeled **R1** and **R2**) by the intensity ratio which depends slightly on the nature of the solvent. The 1,2-Me_2Im resonances are sharp in both sets. This NMR pattern is in agreement with slow rotation of the lopsided 1,2-Me_2Im about the Ru−N bond between two different orientations to produce two diastereotopomers, **R1** and **R2**. Moreover, there are two resolved resonances for Hα and for $(CH_3)\beta$ in both **R1** and **R2**; these are rather narrow for **R1** but broad for **R2**. Since no further splitting

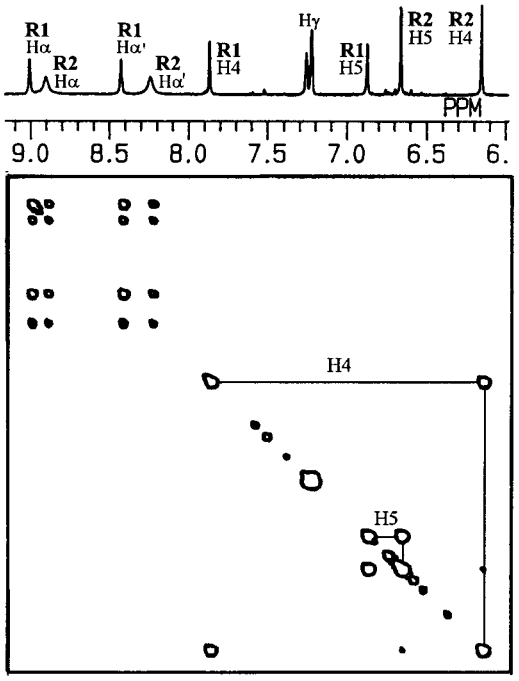

Figure 3. Downfield region of the 2D ^{1}H−^{1}H EXSY spectrum at 20 °C (400 MHz, $CDCl_3$) of *cis,cis,cis*-$RuCl_2(Me_2SO)_2$(3,5-lut)(1,2-Me_2Im).

of NMR resonances was observed, 3,5-lut must be rotating by 180° between two degenerate orientations (topomerization). In $CDCl_3$ solution the slow exchange limit for the rotation of 3,5-lut was reached for both diastereotopomers at −30 °C.

The presence at room temperature of a strong EXSY cross-peak (Figure 3) between each resonance of **R1** and the corresponding resonance of **R2** established the dynamic behavior of **2**. Moreover, each Hα resonance is related by exchange cross-peaks to the other three Hα resonances (Figure 3), indicating contemporaneous rotation of both N-ligands. Rotation of each 3,5-lut about the Ru−N bond exchanges Hα with Hα′ within **R1** and **R2**, while contemporaneous rotation of 1,2-Me_2Im exchanges Hα of **R1** with Hα of **R2**. A similar exchange pattern was found for the resonances of $(CH_3)\beta$.

Discussion

The COSY and NOE connectivity paths from spectra in $CDCl_3$ solution allowed us to assign all the signals of **2** unambiguously (Table 3). The shift of the H(4) resonance of 1,2-Me_2Im is very different for **R1** and **R2** (7.81 ppm in **R1** vs 6.10 ppm in **R2**), suggesting that this proton experiences rather different magnetic environments in the two orientations of this ligand. The 2-Me resonance also exhibits extensive dispersion (1.61 ppm in **R1** vs 2.92 ppm in **R2**). This relationship in the 2-Me shift between rotamers is opposite to that of the H(4) shift. In fact, in **R1**, where the resonance of H(4) occurred at its "normal" downfield frequency, the resonance of 2-Me was anomalously shifted upfield, while the opposite was found for **R2**. In contrast, the resonances of H(5) and 1-Me are considerably less dispersed in the two rotamers.

The ^{1}H NMR chemical shift dispersion of **2** in solution can be explained only if the orientations of 3,5-lut and 1,2-Me_2Im are very similar in solution and in the solid state; our reasoning can be understood best by viewing the rotamers along the Ru−N bond of 1,2-Me_2Im (Figure 4). It is apparent that the only protons with significantly different relationships to other ligands are H(4), H(5), and 2-Me of 1,2-Me_2Im; only signals of these

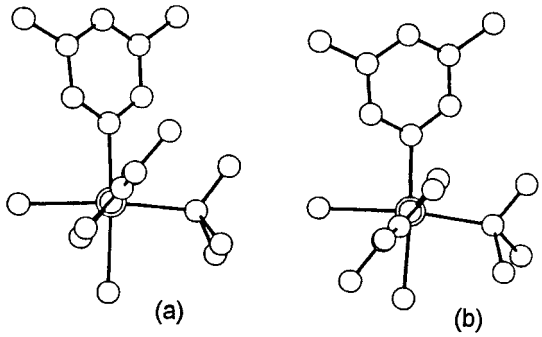

Figure 4. Perspective drawing of *cis,cis,cis*-$RuCl_2(Me_2SO)_2$(3,5-lut)(1,2-Me_2Im) along the Ru−N bond of 1,2-Me_2Im. The two orientations assumed by 1,2-Me_2Im are shown: (a) **R1**; (b) **R2**.

protons shift significantly between **R1** and **R2**. In the more abundant rotamer in the solid, 2-Me is in the shielding cone of the 3,5-lut ring. Therefore, this rotamer is **R1** with the upfield 2-Me signal. In the other solid-state rotamer, the 1,2-Me_2Im H(4) and H(5) fall into this shielding cone, consistent with the upfield H(4) and H(5) signals of **R2**; since H(5) is directed to the periphery of the complex, its resonance is shifted relatively less upfield. At room temperature, the relative abundance of rotamers **R1** and **R2** found in DMSO-d_6 (0.7:0.3) and acetone-d_6 (0.6:0.4) agrees with the ratio found in the solid. Crystallization occurred from a relatively polar solvent environment; thus, the solid-state distribution and structures reflect the solution equilibrium position and structures.

The chemical shifts of 1,2-Me_2Im of **2** can be usefully compared to those of the 1,2-Me_2Im occupying the same position (i.e. trans to Me_2SO) in *cis,cis,cis*-$RuCl_2(Me_2SO)_2(1,2\text{-}Me_2Im)_2$ (**3**).[3] First, the reasonably good agreement found between **R1** of **2** and **R1** and **R4** of **3** and between **R2** of **2** and **R2** and **R3** of **3** (Table 4) suggests that the 1,2-Me_2Im trans to Me_2SO has very similar orientations in the corresponding rotamers of the two complexes. More precisely, the 1,2-Me_2Im trans to Me_2SO of *cis,cis,cis*-$RuCl_2(Me_2SO)_2(1,2\text{-}Me_2Im)_2$ should be oriented with 2-Me pointing toward 1,2-Me_2Im trans to Cl in **R1** and **R4**, while it should be rotated by ∼180° in **R2** and **R3**. This conclusion is in perfect agreement with the orientation predicted by us on the basis of NMR data.[3]

Second, the chemical shifts of H(4) and 2-Me of 1,2-Me_2Im trans to Me_2SO are particularly sensistive to the nature of the cis aromatic N-donor ligand, L1 (Table 4); in particular when H(4) and 2-Me are oriented toward L1. For example, when 2-Me of 1,2-Me_2Im is pointing toward a cis 3,5-lut (**R1** of **2**), it is considerably more deshielded compared to when it is pointing toward a cis 1,2-Me_2Im (**R1** and **R4** of **3**); the same happens for H(4). It can be concluded that 3,5-lut is more anisotropic than 1,2-Me_2Im. Moreover, the anisotropy of the 1,2-Me_2Im ring is lopsided; in fact, H(4) (or 2-Me) is more deshielded when it is pointing toward the $C_4{=}C_5$ side of the cis 1,2-Me_2Im molecule (**R3** of **3**) compared to when it is oriented toward the 2-Me side of the same ligand (**R2** of **3**).

In $CDCl_3$ solution, the **R1**:**R2** ratio (0.4:0.6) gradually increased as the temperature was lowered and the two rotamers were almost equally abundant at −30 °C. From the thermodynamic parameters estimated from VT NMR data for the **R1** to **R2** equilibrium (ΔH = 1.1 kcal/mol, ΔS = 4.7 cal/K·mol), conformer **R1** is enthalpically slightly favored, while **R2** is entropically favored. The kinetics for 3,5-lut rotation about the Ru−N bond in both rotamers were evaluated with the width at half-height of the Hα resonances from −10 to +40 °C.[9] The 3,5-lut rotation rate of **R1** was one-tenth that of **R2**. A $\Delta G^{\ddagger}$ of 16.5 ± 0.1 kcal/mol was found for the "slow" rotamer **R1**, compared with 15.3 ± 0.1 kcal/mol for the "fast" rotamer **R2**. From the NMR data, an obvious explanation for these rate differences is that the 2-Me group in **R1** increases steric barriers to the 3,5-lut rotation. However, we note that the difference in rotation barrier between rotamers of only ∼1 kcal/mol seems low if one considers models in which the two rotamers have more or less normal coordination geometries. The unusual finding that both rotamers are present in the same solid environment allows us to assess this issue with structural details not normally available. Furthermore, the rotamers allow us to understand forces within the coordination sphere; these are worth understanding since cis arrangements of heterocycles occur widely in metallobiochemistry.

With the addition of the new solid-state data for compounds of the type *cis,cis,cis*-$RuCl_2(Me_2SO)_2$(L1)(L2), there is now a large enough database for assessing the finer structural features of the rotamers. We begin with the *cis,cis*-$RuCl_2(Me_2SO)_2$ moiety, which is surprisingly similar in structure given the expected relatively free rotation around the Ru−S bond. In all cases,[3,4] the oxygens of the Me_2SO ligands point away from the other ligands. The methyl groups of each Me_2SO straddle a Ru−Cl bond in such a way that one Me lies above and constricts the adjacent L. In **1** and **2** nonbonding distances in the range 3.07−3.32 Å were found between these methyls and the adjacent L. The NMR data suggests that this arrangement predominates in solution since for each Me_2SO one Me signal is shifted upfield, a finding consistent with the relationship of the Me groups with respect to the anisotropic L group.

As a consequence, the arrangement creates a restriction forcing the L ligands into a limited spacial zone. In complex **1** the two bases are slightly tilted toward each other. The tilt is such that the Ru atom lies ∼0.3 Å out of the mean plane of each L ligand. In complex **2**, 1,2-Me_2Im is displaced toward 3,5-lut in **R2** (N(1)−Ru−N(2) angle 78.1(3)° in **R2** vs 93.5(2)° in **R1**; N(1)−N(2a) nonbonding distance 2.71 Å in **R2** vs N(1)−N(2) 3.08 Å in **R1**). This movement, which should also occur in solution, will increase the steric barrier in **R2** compared to an undistorted **R2** and explain the relatively small difference in kinetic parameters for 3,5-lut rotation between **R1** and **R2**. The major factor causing the movement appears to be repulsion between the 2-Me group and the two Cl's. This 2-Me group also appears to cause steric problems for the major rotamer **R1** since the angles N(1)−Ru−N(2) and S(1)−Ru−N(2) are larger than in **1** and in the other related compounds.[3,4]

Analysis of the solution dynamic behavior of *cis,cis,cis*-$RuCl_2(Me_2SO)_2$(L1)(L2) complexes allows us to rank the L ligands according to their steric bulk. For example, in both *cis,cis,cis*-$RuCl_2(Me_2SO)_2$(py)(Me_3Bzm) and *cis,cis,cis*-$RuCl_2(Me_2SO)_2$(3,5-lut)(1,2-Me_2Im) the six-membered ring py or 3,5-lut ligand trans to Cl rotates about the Ru−N bond at a slow-to-intermediate rate on the NMR time scale; slow rotation is reached at comparable temperatures, −40 °C for py[4] and −30 °C for 3,5-lut. Assuming that py and 3,5-lut have a similar steric demand, their rotation rate is influenced only by the nature of the cis L ligand; therefore, 1,2-Me_2Im (both orientations) and Me_3Bzm provide a roughly comparable steric barrier to rotation but one which is larger than that of py and 3,5-lut. In fact, when the position trans to Cl is occupied by Me_3Bzm or 1,2-Me_2Im, i.e., in *cis,cis,cis*-$RuCl_2(Me_2SO)_2(Me_3Bzm)_2$ and *cis,*-

(9) Sandström, J. *Dynamic NMR Spectroscopy*; Academic Press: London, 1982.

cis,cis-$RuCl_2(Me_2SO)_2(1,2\text{-}Me_2Im)_2$, respectively, rotation of such ligands is already slow at room temperature. In *cis,cis,cis*-$RuCl_2(Me_2SO)_2(1,2\text{-}Me_2Im)_2$ the 1,2-Me_2Im trans to Cl cannot flip back and forth in the rotamer with the 2-Me group of 1,2-Me_2Im trans to Me_2SO pointing toward it.[3] In contrast, the 3,5-lut trans to Cl can flip back and forth regardless of the orientation of the 1,2-Me_2Im in *cis,cis,cis*-$RuCl_2(Me_2SO)_2$(3,5-lut)(1,2-Me_2Im). This result shows that 3,5-lut is less sterically demanding than 1,2-Me_2Im.

Finally, we note that in both **1** and **2** only one of the two possible geometrical isomers was observed. However, 1,2-Me_2Im is trans to Cl in **1**, while it is trans to Me_2SO in **2**. While the geometry of **2** appears to be dictated by steric factors, i.e., the more sterically demanding 1,2-Me_2Im ligand is in the less sterically crowded position trans to Me_2SO, the same motif does not seem to apply in the case of **1**, where both L ligands have comparable steric hindrance and a mixture of the two geometrical isomers might be expected. The question arises why a relatively bulky ligand such as Me_3Bzm, given the choice, always selectively occupies the coordination site trans to Me_2SO, where it is then unable to rotate. The similarly bulky 1,2-Me_2Im ligand is nevertheless able to rotate when bound in the same position. The X-ray structure of **1** demonstrates that the orientation of the Me_3Bzm trans to Me_2SO is very similar to that found for the corresponding ligand in *cis,cis,cis*-$RuCl_2(Me_2SO)_2$(py)(Me_3Bzm) and *cis,cis,cis*-$RuCl_2(Me_2SO)_2(Me_3Bzm)_2$, with H(2) on C(16) pointing between the Cl atoms. These observations reveal the role of the electrostatic interactions between the δ^+ H(2) of Me_3Bzm and the cis chlorides and lead us to formulate the following working hypothesis: in *cis,cis,cis*-$RuCl_2(Me_2SO)_2$(L1)(L2) complexes, when a ligand, such as Me_3Bzm, is capable of giving favorable electrostatic interactions with the two cis halides, both the ligand position and its orientation are mainly determined by such forces, regardless of the bulkiness of the ligand. When interligand electrostatic interactions are less relevant, such as with 1,2-Me_2Im, steric factors determine disposition and orientations of L ligands. In such cases, conformer distribution was successfully simulated by molecular mechanics calculations.[10]

Conclusions

The crystal structure of *cis,cis,cis*-$RuCl_2(Me_2SO)_2$(1,2-Me_2Im)(Me_3Bzm) (**1**) confirms the geometry previously established by NMR.[3] As in previous examples, the orientation of ligands in the solid-state structure corresponds to that of the most abundant rotamer in solution. Instead, *cis,cis,cis*-$RuCl_2(Me_2SO)_2$(3,5-lut)(1,2-Me_2Im) (**2**) provides a rare example in which the solid state closely reflects the solution state, both in the structure of species involved in a conformational equilibrium and in the position of that equilibrium. Thus, we are able to gain structural information on both the less stable and the more stable rotamers in the same solid-state environment. Combined with previous structural studies, these results suggest that the *cis,cis*-$RuCl_2(Me_2SO)_2$ moiety generally adopts a very similar arrangement regardless of the nature of the two L ligands. The two rotamers of *cis,cis,cis*-$RuCl_2(Me_2SO)_2$(3,5-lut)(1,2-Me_2Im) both appear to be strained with 1,2-Me_2Im occupying a slightly unusual location in both rotamers; the strain in both decreases the energy difference and probably accounts for the similar dynamic behaviors of 3,5-lut in the two rotamers.

Additional examples of crystallographically characterized unstable conformers would be valuable to study, especially if complementary data are available for the stable form. In this study, the unstable rotamer has structural features which suggest that two cis heterocyclic ligands can be forced together in response to forces within the coordination sphere.

Acknowledgment. We thank the NIH (Grant GM 29222) and Italian MURST for support and Johnson Matthey for a loan of hydrated $RuCl_3$. The NSF (Grant ASC-9527186) supported remote collaborative research by the Internet.

Supporting Information Available: Rate constants and free energies of activation ($\Delta G^{\ddagger}$) for 3,5-lut rotation in **2** (1 page). Two X-ray crystallographic files, in CIF format, are available. Ordering access information is given on any current masthead page.

IC980066J

(10) Geremia, S.; Calligaris, M. *J. Chem. Soc., Dalton Trans.* **1997**, 1541.